Available online at www.sciencedirect.com
SCIENCE DIRECT®
Journal of Magnetic Resonance 163 (2003) 46–55
JMR Journal of Magnetic Resonance
www.elsevier.com/locate/jmr

Separated local field spectroscopy of columnar and nematic liquid crystals

Sergey V. Dvinskikh,[a,*] Herbert Zimmermann,[b] Arnold Maliniak,[a] and Dick Sandström[a]

[a] *Division of Physical Chemistry, Arrhenius Laboratory, Stockholm University, SE-10691 Stockholm, Sweden*
[b] *Department of Biophysics, Max-Planck-Institut für Medizinische Forschung, Jahnstrasse 29, D-69120 Heidelberg, Germany*

Received 21 November 2002; revised 21 January 2003

Abstract

We are in this work comparing the efficiencies of various ^{1}H–^{13}C separated local field (SLF) experiments when applied to columnar and nematic liquid crystals. In particular, the performances of the conventional SLF, proton-detected local field (PDLF), and polarization inversion spin exchange at the magic angle (PISEMA) methods in terms of spectral resolution, robustness, and ability to measure long-range couplings are investigated. The PDLF sequence provides in most cases the best dipolar resolution. This is especially obvious for weakly coupled ^{1}H–^{13}C spin pairs.
© 2003 Elsevier Science (USA). All rights reserved.

Keywords: Separated local field spectroscopy; Dipolar couplings; PDLF; PISEMA; Liquid crystals

1. Introduction

Two-dimensional (2D) separated local field (SLF) NMR spectroscopy is one of the most powerful techniques to measure and assign heteronuclear dipolar couplings. In macroscopically oriented samples, which include single crystals, liquid crystals, and biomolecules in lipid bilayers, magic-angle spinning (MAS) is not required for obtaining high spectral resolution. For these samples, site-resolved dipolar splittings can be observed in 2D SLF experiments without the complications imposed by MAS. A variety of SLF methods have been introduced. In the conventional SLF technique [1] with homonuclear ^{1}H–^{1}H interactions suppressed, the rare spins (usually ^{13}C) evolve under the influence of dipolar local fields produced by the surrounding protons. This results often in crowded and poorly resolved multiplet spectra. Recently, more advanced NMR experiments have been developed which yield simpler spectra with higher resolution [2–10]. In proton-detected local field (PDLF) techniques [2–6, 11,12] the spectra are governed by simple two-spin interactions because the dipolar field is probed at the abundant spins (^{1}H) rather than at the rare spins. This results in a dramatic spectral simplification as compared to the situation in traditional SLF spectroscopy since the PDLF spectra consist of a superposition of doublets. Another popular method is the polarization inversion spin exchange at the magic angle (PISEMA) experiment [8]. This sequence combines flip-flop, frequency- and phase-switched Lee–Goldburg homonuclear decoupling [13–15] with cross-polarization (CP). In PISEMA, the dipolar couplings are measured through the transient oscillations taking place during the CP process.

Numerous local field studies of molecular structure and ordering in partially oriented media have been published since the first report in 1979 [16]. Oriented thermotropic liquid crystals have been investigated by both traditional SLF spectroscopy (see reviews [17,18], and references therein) and by PDLF experiments [2,4–6,19–22]. Studies of lyotropic phases by SLF [23] and PDLF methods [2,3,24–26] have also been presented. The PISEMA technique has often been used in conformational studies of biomolecules oriented in liquid-crystalline lamellar environments [10,27–38]. Experiments in

* Corresponding author. On leave from Institute of Physics, St. Petersburg State University, 198904 St. Petersburg, Russia. Fax: +46-8-15-21-87.
E-mail address: sergey@physc.su.se (S.V. Dvinskikh).

1090-7807/03/$ - see front matter © 2003 Elsevier Science (USA). All rights reserved.
doi:10.1016/S1090-7807(03)00058-2

thermotropic liquid crystals based on similar principles as PISEMA have also been reported [39,40]. Recently, various local field methods were applied to columnar mesophases [41].

In this work we compare the efficiencies of various ^{1}H–^{13}C separated local field experiments when applied to columnar and nematic phases. In particular, the performances of the conventional SLF, PDLF, and PISEMA methods in terms of spectral resolution, robustness and ability to measure long-range couplings are investigated. Potential problems due to radio-frequency (RF) heating are also addressed.

2. Pulse sequences

In the conventional SLF sequence, shown in Fig. 1a, CP-enhanced ^{13}C magnetization is allowed to evolve under the ^{1}H–^{13}C heteronuclear dipolar couplings during the variable evolution period t_1. A ^{13}C 180° pulse is applied at t_1 to refocus the ^{13}C chemical shift interaction. The signal is finally observed during the detection period as it evolves under the ^{13}C chemical shift interaction and ^{1}H heteronuclear decoupling. A constant-time version [42] of this experiment was also employed. In this case, the total evolution time τ in the indirect dimension is kept constant and proton heteronuclear decoupling is applied during the interval τ–t_1 with a ^{13}C 180° pulse inserted at $\tau/2$.

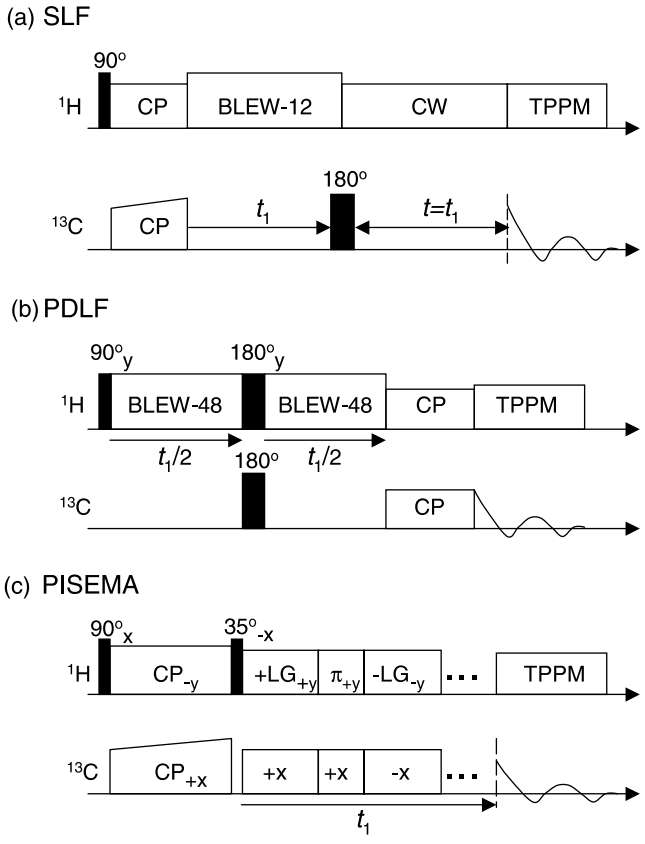

Fig. 1. Pulse sequences for 2D dipolar local field spectroscopy. All experiments correlate scaled ^{1}H–^{13}C dipolar couplings during t_1 evolution with ^{13}C chemical shifts during detection. (a) Conventional SLF spectroscopy. (b) PDLF spectroscopy. (c) PISEMA spectroscopy.

In the PDLF experiment (see Fig. 1b) ^{1}H magnetization is allowed to evolve under the local field of rare ^{13}C spins during t_1. A pair of 180° pulses is applied simultaneously at $t_1/2$ to refocus ^{1}H chemical shifts while retaining the ^{1}H–^{13}C couplings. The signal is then transferred to ^{13}C via CP and finally detected under ^{1}H heteronuclear decoupling.

In both SLF and PDLF spectroscopy it is necessary to remove ^{1}H–^{1}H homonuclear dipolar couplings during the evolution period t_1, and we have compared the efficiencies of several homonuclear decoupling sequences including MREV-8 [43,44], BLEW-12 [45], and BLEW-48 [45]. For our samples using the SLF approach it was found that the sequences BLEW-12 and BLEW-48 performed equally well and provided slightly higher resolution than MREV-8. While better performance is in general expected for the long cycle BLEW-48 sequence [45], the resolution is limited by the intrinsic complexity of the SLF dipolar spectrum. The highest resolution in the PDLF spectra was observed for BLEW-48. In order to increase the spectral width in the dipolar dimension of 2D PDLF spectra, the evolution period was incremented in steps of half of a full BLEW-48 cycle time.

The PISEMA pulse sequence is shown in Fig. 1c. After standard ^{1}H–^{13}C CP, the ^{1}H magnetization is aligned at the magic angle to the static magnetic field by means of a ^{1}H 35° pulse. Then follows the SEMA evolution period in t_1 where the ^{1}H magnetization is spin locked by off-resonance flip-flop Lee–Goldburg irradiation [13–15], and matched by a phase-alternated ^{13}C spin-lock field. The dipolar couplings are monitored through the oscillations resulting from coherent energy transfer between ^{1}H and ^{13}C spins during t_1. As shown in Fig. 1c, 180° pulses may be inserted in basic SEMA cycle to refocus dephasing due to phase transients [9].

In all 2D experiments, the TPPM heteronuclear decoupling scheme [46] was used during the detection period. Only cosine-modulated data sets were collected in t_1 yielding symmetric spectra in the dipolar dimension.

The multiple-pulse scaling factor k for the PDLF sequence was calibrated by observing the scaling of the ^{1}H frequency offset under BLEW-48 irradiation in a HETCOR-type experiment [5]. The experimental value, 0.420, is in good agreement with the theoretical counterpart 0.424 [45]. For the SLF method using BLEW-12 and for PISEMA the theoretical values for the scaling factor, 0.475 [45] and 0.816 [8], respectively, were assumed.

3. Results

We now describe and analyze the 2D spectra obtained using the above-mentioned NMR methods. Two discotic samples, hexapentyloxy-triphenylene (THE5) and 1,2,3,5,6,7-hexaoctyloxy-rufigallol (RufH8O), were studied. The molecular structures of these compounds are shown in Figs. 2a and b. The THE5 sample was deuterated in the aliphatic side chains and RufH8O was ^{13}C enriched to 10% in the α methylene positions.

Both THE5 and RufH8O form hexagonal columnar phases over a wide temperature range [47,48]. The phase transition temperatures are indicated in Fig. 2. In the mesophase, the molecules undergo fast reorientation about the columnar axes. The experiments discussed below were carried out on stationary samples oriented in the magnetic field of the NMR spectrometer by slowly cooling from the isotropic phase. This procedure results in a distribution of domains in which all columns are aligned perpendicular to the magnetic field.

In addition to the discotic samples, we have also studied the mesogenic molecule 4-*n*-pentyl-4′-cyanobiphenyl (5CB, see Fig. 2c) in the nematic phase which orients spontaneously along the magnetic field of the spectrometer.

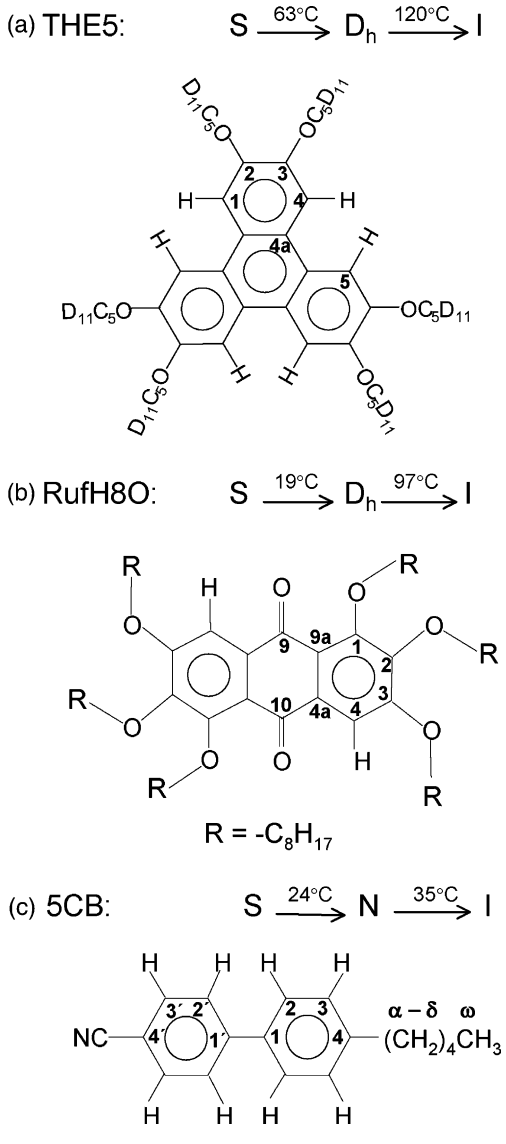

Fig. 2. Molecular structures of: (a) chain-deuterated hexapentyloxy-triphenylene (THE5), (b) 1,2,3,5,6,7-hexaoctyloxy-rufigallol (RufH8O), and (c) 4-*n*-pentyl-4′-cyanobiphenyl (5CB). The phase diagrams of these compounds are also included: S, D_h, N, and I stand for solid, hexagonal columnar, nematic, and isotropic liquid phases, respectively.

3.1. THE5

Fig. 3a shows the conventional proton-decoupled ^{13}C CP spectrum of chain-deuterated THE5 in the columnar phase. The three non-equivalent core carbons produce the aromatic signals. The previously reported [47] spectral assignment indicated in Fig. 3a is confirmed by the 2D PDLF experiment discussed below. The quintet with intensity distribution 1:2:3:2:1 in the aliphatic region corresponds to the α carbon signal split by dipolar couplings to the deuterons in the α methylene group. The remaining methylene signals are not resolved due to multiple dipolar couplings to ^2H spins.

Dipolar cross-sections extracted from 2D SLF, PDLF, and PISEMA spectra of THE5 are shown in Fig. 3b. The strong coupling between C_4 and its directly bonded proton is well resolved in all sub-spectra with splittings of 9.10, 9.40, and 9.40 kHz (corrected for the multiple-pulse scaling) for the SLF, PDLF, and PISEMA experiments, respectively. The resolution of the main dipolar coupling in the PDLF and PISEMA slices of C_4 is comparable with linewidths of 260 and 190 Hz, respectively. The corresponding dipolar linewidth in the conventional SLF spectrum is around 700 Hz. Note also that the C_4 PDLF cross-section displays a clearly resolved smaller splitting of 730 Hz which can be ascribed to the dipolar coupling to the next nearest proton H_5 in the triphenylene core. This coupling is also seen in the SLF spectrum of C_4 as a 740 Hz fine splitting of the main doublet. No analogous feature is observed in the C_4 PISEMA slice.

The PDLF experiment provides superior resolution for the slices through C_3 and C_{4a}. Two doublets with splittings equal to 1260 and 620 Hz are observed in the C_{4a} cross-section, while the sub-spectrum through C_3 exhibits one splitting of 1350 Hz. These doublets arise from the dipolar couplings $^1H_4$–$^{13}C_{4a}$, $^1H_5$–$^{13}C_{4a}$, and $^1H_4$–$^{13}C_3$, respectively. The zero-frequency peaks originate from unresolved long-range heteronuclear couplings. Only partially resolved dipolar doublets are observed in the conventional SLF spectra with splittings of around 1500 and 1300 Hz for C_{4a} and C_3, respectively. The corresponding cross-sections through the 2D

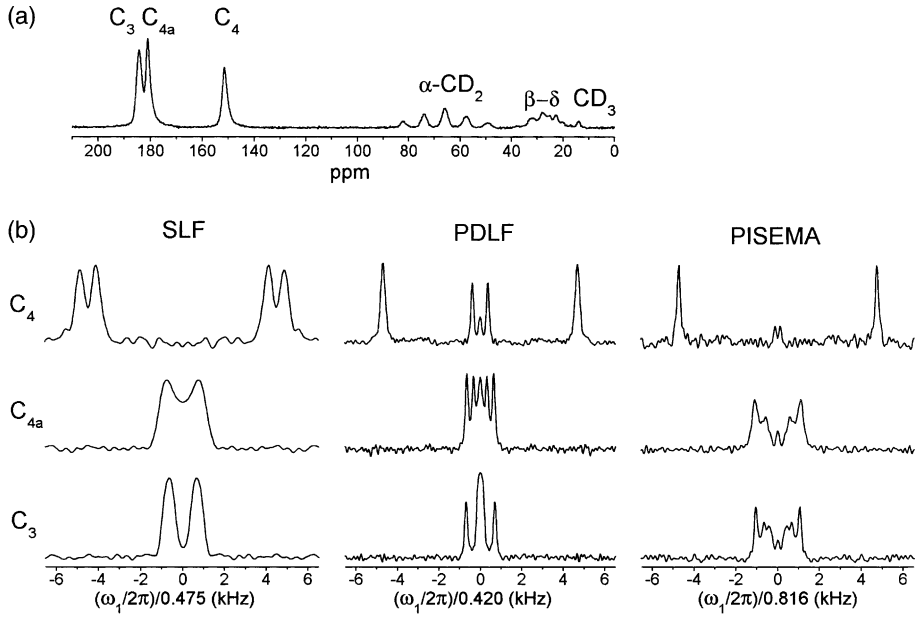

Fig. 3. NMR spectra of chain-deuterated THE5 in the columnar phase at 110 °C. (a) Carbon-13 CP spectrum. (b) Dipolar cross-sections through 2D SLF, PDLF, and PISEMA spectra. Note that the ω_1 frequency axes are corrected by the multiple-pulse scaling factors. The CP contact time was 2 ms in the PDLF experiment. The PISEMA spectrum was obtained without the refocusing 180° pulses in the SEMA cycle. The 2D spectra were acquired using 80 t_1 increments of 79.2 μs (SLF), 100 t_1 increments of 158.4 μs (PDLF), and 100 t_1 increments of 65.2 μs (PISEMA).

PISEMA spectrum exhibit complex lineshapes which are difficult to analyze. It was also found that these spectra are highly sensitive to the ^{1}H carrier offset, and whether or not the refocusing 180° pulses are inserted in the SEMA cycle.

The one-bond $^1H_4$–$^{13}C_4$ dipolar coupling is readily interpreted in terms of molecular ordering. If we take into account the orientation of the columnar phase, the core splitting $\Delta\nu$ may be written as [18]

$$\Delta\nu = \left|\frac{1}{2}SD_{CH}\right|, \tag{1}$$

where

$$D_{CH} = -\frac{\mu_0}{8\pi^2}\frac{\gamma_C\gamma_H\hbar}{r_{CH}^3} \tag{2}$$

is the ^{1}H–^{13}C dipolar coupling constant, S is the orientational order parameter, and r_{CH} is the spin–spin distance. The other symbols have their usual meanings [42]. Using a heteronuclear spin–spin distance of $r_{CH} = 1.09$ Å, a value of $D_{CH} = -23.3$ kHz is obtained. The $^1H_4$–$^{13}C_4$ dipolar splitting in the C_4 cross-section is equal to 9.40 kHz (see Fig. 3b), and employing Eq. (1) we find that the order parameter is 0.81 at 110 °C. The contribution from the small isotropic J_{CH} coupling (of the order of 150 Hz) was neglected in this calculation. This order parameter in combination with standard bond lengths may be used to estimate the dipolar splittings $^1H_5$–$^{13}C_4$, $^1H_4$–$^{13}C_{4a}$, $^1H_5$–$^{13}C_{4a}$, and $^1H_4$–$^{13}C_3$, and employing Eq. (1) once more we find the following values: 680, 1190, 590 and 1320 Hz, respectively. These numbers are in good agreement with the observed splittings in the PDLF spectrum (730, 1260, 620, and 1350 Hz, respectively, see above) and verify the assignment of the aromatic ^{13}C NMR signals. Since weak dipolar couplings originate from indirectly bonded nuclei, the corresponding J_{CH} couplings are small (typically below 15 Hz) and can be neglected.

One may argue that the high dipolar resolution observed for THE5 is a consequence of the low proton concentration in this heavily deuterated liquid crystal. Therefore, we are presenting local field spectra of fully protonated samples below.

3.2. RufH8O

Fig. 4a shows the proton-decoupled ^{13}C CP spectrum of RufH8O-10%-$^{13}C_\alpha$ in the columnar phase. The core and α methylene resonances were assigned by a variety of NMR techniques, and the details of these measurements will be presented in a forthcoming communication.

Dipolar cross-sections from a 2D PDLF spectrum of RufH8O-10%-$^{13}C_\alpha$ obtained at 85 °C are shown in Fig. 4b. Each slice consists of a superposition of doublets due to the pair-wise ^{1}H–^{13}C couplings. In order to facilitate the observation of weak spin–spin interactions, the spectrum was obtained by using a relatively long (4 ms) CP contact time. The spectral resolution is high for both aromatic and aliphatic signals with dipolar linewidths comparable to those obtained for chain-deuterated THE5. The splittings in the aromatic region result from

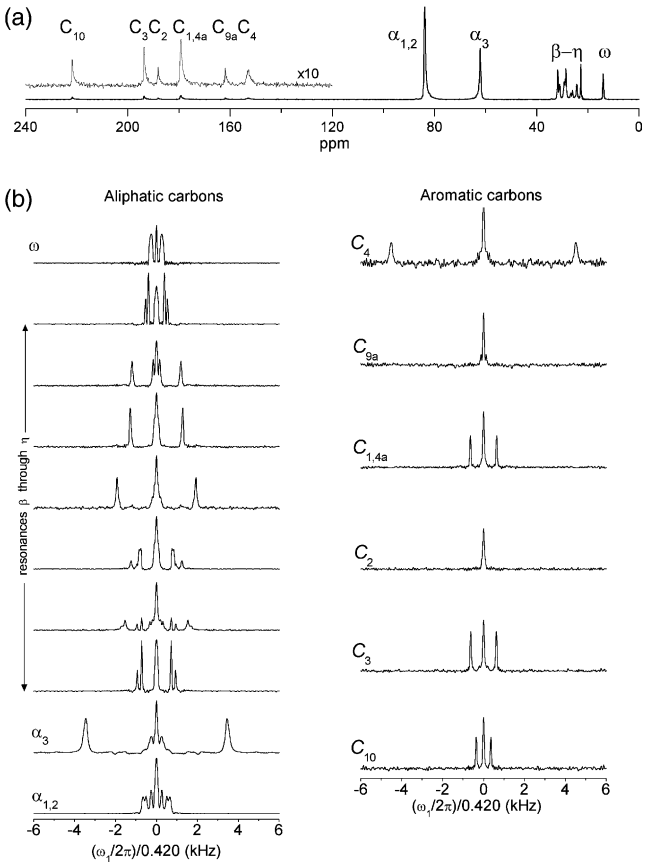

Fig. 4. Spectra of RufH8O-10%-$^{13}C_\alpha$ in the columnar phase at 85 °C. (a) Carbon-13 CP spectrum. (b) Dipolar cross-sections through a 2D PDLF spectrum. Note that the ω_1 frequency axis has been corrected by the multiple-pulse scaling factor. The CP contact time was 4 ms. The 2D spectrum was acquired using 100 t_1 increments of 158.4 μs. The assignment of C_1 and C_2 is uncertain.

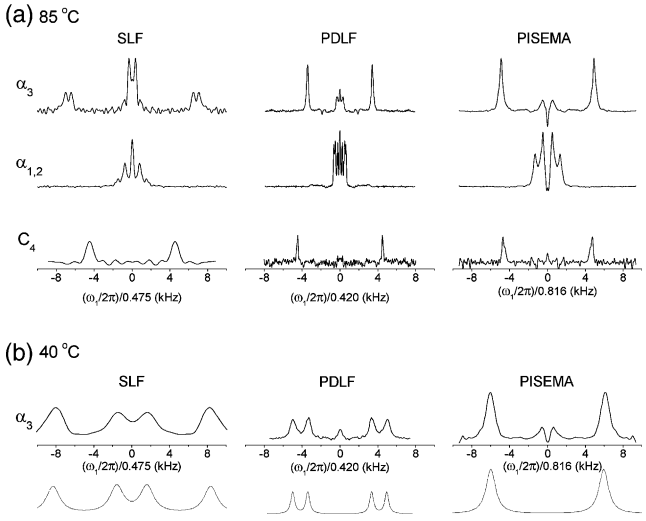

Fig. 5. Dipolar slices through 2D SLF, PDLF and PISEMA spectra of RufH8O-10%-$^{13}C_\alpha$ in the columnar phase. All ω_1 frequency axes have been corrected by the multiple-pulse scaling factors. The CP contact time was 2 ms in the PDLF experiments. The PISEMA spectra were obtained without the refocusing 180° pulses in the SEMA cycle. (a) Spectra obtained at 85 °C. The constant-time version of the SLF sequence was employed. The signal from the aromatic C_4 carbon has a rapid T_2 decay, and was therefore recorded using a short constant-time delay ($\tau/2$) of 1.9 ms (corresponding to, in total, 16 t_1 increments of 118.8 μs). The α methylene signals were recorded with $\tau/2 = 7.9$ ms (100 t_1 increments of 79.2 μs). The 2D PDLF and PISEMA spectra were recorded with 100 t_1 increments of, respectively, 158.4 and 65.2 μs. (b) Spectra obtained at 40 °C. The constant-time SLF sequence was used with $\tau/2 = 2.4$ ms (60 t_1 increments of 39.6 μs). The 2D PDLF and PISEMA spectra were recorded with 64 t_1 increments of, respectively, 158.4 and 32.6 μs. In the lineshape simulations (thin lines), the ^{1}H–^{13}C dipolar couplings D_1 and D_2 were set to 3.4 and 5.0 kHz, respectively.

couplings between core carbons and H_4. As expected, the C_4 slice exhibits the largest splitting (9.04 kHz) due to the one-bond $^1H_4$–$^{13}C_4$ dipolar interaction, and using Eq. (1) we obtain an orientational order parameter of 0.78 at 85 °C. Several smaller splittings of the core signals are also visible in Fig. 4b. In particular, we observe splittings for resonances C_3, C_{4a}, and C_{10} with values of 1240, 1290 and 710 Hz, respectively. The calculated counterparts, using standard values for bond lengths and an order parameter of 0.78, are 1190, 1260 and 710 Hz, respectively. For the remaining core carbons the calculated splittings are $\leqslant 200$ Hz, and are consequently not resolved in the experimental sub-spectra.

The ^{13}C chemical shifts of the α methylene groups indicate that the side chains are structurally and/or dynamically nonequivalent (see Fig. 4a) [41]. This nonequivalence manifests itself also in the $^1H_\alpha$–$^{13}C_\alpha$ couplings: the largest dipolar splitting in the α_3 slice is 6.90 kHz, while the splittings for the other two α methylenes are much smaller (cf. Fig. 4b).

Representative cross-sections of RufH8O-10%-$^{13}C_\alpha$ obtained at 85 °C using the SLF, PDLF, and PISEMA methods are shown in Fig. 5a. The spectral resolution of the PDLF sequence is better than those of the other experiments. As expected for a CH_2 group, the main feature of the α_3 SLF slice is a 1:2:1 triplet with line splittings equal to $2D$ (where $D = 3.40$ kHz is the residual one-bond ^{1}H–^{13}C coupling). In accordance with theory [2,49], the PDLF and PISEMA spectra of α_3 exhibit doublets with splittings of $2D$ and $2\sqrt{2}D$, respectively. Each component in the α_3 SLF triplet is in turn split by the core proton H_4 into a doublet with a separation of 660 Hz. This coupling also explains the inner splitting of 640 Hz in the PDLF cross-section. Note that the PISEMA experiment is insensitive to weak ^{1}H–^{13}C dipolar interactions in the presence of stronger ones (see, e.g., the α_3 slice in Fig. 5a). Weak couplings merely cause small peak shifts, line broadening and zero-frequency artifacts [49].

The strong $^1H_4$–$^{13}C_4$ dipolar coupling is well resolved in all spectra with a splitting of 9.04 kHz for both the SLF and PDLF slices. A slightly larger splitting of 9.40 kHz is observed in the PISEMA spectrum. The discrepancy between these numbers probably stems

from a combination of the ^{1}H resonance offset effect and the influence from long-range heteronuclear couplings in the PISEMA experiment (see below).

At lower temperatures, the local field NMR spectra of RufH8O-10%-$^{13}C_\alpha$ exhibit some unexpected features. This is illustrated in the top row of Fig. 5b which shows α_3 slices obtained at 40 °C. Two doublets are observed in the PDLF cross-section, while the PISEMA spectrum consists of only one doublet. The SLF slice is composed of four signals. These lineshapes may be explained by assuming that the two CH bond vectors in the α_3 methylene group have different orientations with respect to the core rotation axis. This results in two non-equivalent dipolar couplings, D_1 and D_2, within the α_3 methylene fragment, and leads to two doublets in the PDLF experiment. This model also accounts for the doublet-of-a-doublet feature in the SLF slice and the single PISEMA doublet with a splitting of $2\sqrt{D_1^2 + D_2^2}$ [49]. As shown in the bottom row of Fig. 5b, simulations based on this model are in agreement with the experimental lineshapes. The implications of these non-equivalent couplings in terms of molecular structure are addressed elsewhere [41].

3.3. 5CB

Fig. 6a shows the proton-decoupled ^{13}C spectrum of 5CB in the nematic phase. The peak assignment was taken from the literature [17]. Dipolar cross-sections using the three local field methods are displayed in Fig. 6b. The PDLF experiment provides again superior spectral resolution with dipolar linewidths one order of magnitude smaller than those observed in the SLF slices.

The conventional SLF cross-sections in Fig. 6b resemble previously reported SLF dipolar spectra obtained under off-magic-angle spinning (OMAS) conditions [6]. It is clear that this method only resolves the largest couplings.

PDLF spectra of 5CB have in the past been acquired under both static [4] and OMAS conditions [4–6], with results similar to the one shown in the central column of Fig. 6b. The dipolar resolution is, however, somewhat better in our experiment compared to those reported previously. This probably stems from (i) the use of the more efficient BLEW-48 irradiation instead of the MREV-8 sequence [4,5], (ii) the use of higher decoupling power in BLEW-48 irradiation as compared to [6], and (iii) the absence of the dipolar scaling due to the sample spinning. In addition to the large dipolar splittings, a number of smaller ones is also resolved in each ^{13}C cross-section. The assignment of some of these long-range couplings has been reported elsewhere [4–6,19]. Note that the resolution in the PDLF spectrum is high for both the aromatic and aliphatic regions in spite of large differences in the dipolar splittings and ^{1}H chemical shifts.

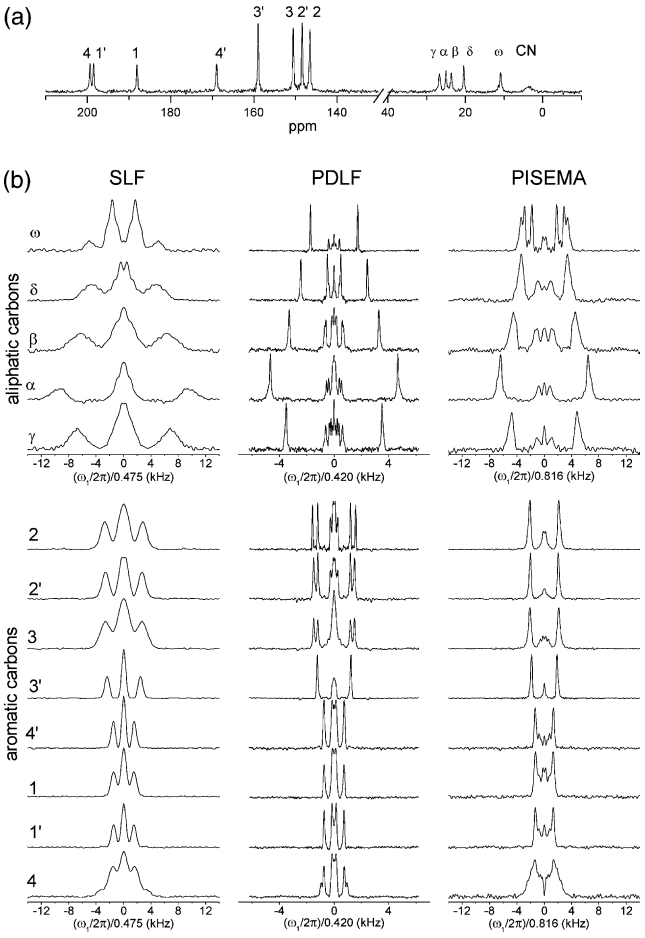

Fig. 6. NMR spectra of 5CB in the nematic phase at 20 °C. (a) Carbon-13 spectrum obtained by single pulse excitation. (b) Dipolar cross-sections through 2D SLF, PDLF, and PISEMA spectra. The ω_1 frequency axes have been corrected by the multiple-pulse scaling factors. The CP contact time was 1 ms in the PDLF experiment. The PISEMA spectra were recorded with the refocusing 180° pulses in the SEMA cycle. The aromatic and aliphatic PISEMA signals were obtained from two separate experiments in which the ^{1}H resonance offset was optimized for either the aliphatic or the aromatic signals. The 2D spectra were acquired with, respectively, 80 t_1 increments of 48.0 μs (SLF), 100 t_1 increments of 192.0 μs (PDLF), and 100 t_1 increments of 40.75 μs (PISEMA). Note that the scale of the frequency axis of the PDLF spectrum is expanded by a factor of 2 compared to those of SLF and PISEMA.

In order to obtain reasonable resolution in the PISEMA slices it was necessary to perform two separate experiments in which the ^{1}H resonance offset was optimized for either the aliphatic or the aromatic signals. A few of the biphenyl resonances in the PISEMA cross-sections exhibit dipolar linewidths that are comparable to those observed in the PDLF experiment. However, the resolution in the chain region of the PISEMA spectrum is clearly inferior as compared to the PDLF experiment. A drawback associated with PISEMA spectroscopy is that a ^{13}C spin coupled to two non-equivalent protons produces a single doublet with a splitting of $2\sqrt{D_1^2 + D_2^2}$. This property makes it

impossible to extract the two individual dipolar couplings. In contrast, such a three-spin system yields in PDLF spectroscopy two doublets with splittings equal to $2D_1$ and $2D_2$, respectively. An example of this kind of spin cluster was already encountered in the low-temperature spectra of RufH8O (see Fig. 5b). The same type of behavior is observed in, e.g., the PDLF and PISEMA slices through the C_3 site in 5CB (see Fig. 6b). In accordance with theory [49], the methyl signal in the PISEMA spectrum consists of three doublets with relative splittings of $1{:}\sqrt{3}{:}2$.

The one-bond couplings obtained from the three 2D local field spectra are in good agreement with each other. For example, the strong $^1H_\alpha$–$^{13}C_\alpha$ dipolar interaction estimated from SLF, PDLF, and PISEMA cross-sections are $\Delta\nu/4 = 4.60$, $\Delta\nu/2 = 4.68$, and $\Delta\nu/(2\sqrt{2}) = 4.55$ kHz, respectively, where $\Delta\nu$ denotes the distance between the outer peaks in the corresponding spectra.

4. Discussion and conclusions

4.1. Resolution of dipolar couplings

For the three liquid-crystalline samples studied in this work, the PDLF and PISEMA techniques provide significantly better spectral resolution as compared to the conventional SLF sequence. In some cases, the dipolar linewidths of conventional SLF spectra can be decreased if a constant-time experiment is performed. Yet, the SLF resolution cannot compete with that offered by PDLF and PISEMA. The resolution in the SLF method is limited by the multiplet-type nature of the SLF dipolar spectrum where each additional proton contributes with a successive first-order splitting.

In PISEMA spectroscopy, weak heteronuclear couplings are truncated in the presence of a strongly coupled ^{1}H–^{13}C spin pair [49]. The remote protons do not cause any observable splittings of the main doublet but result merely in small peak shifts, limited line broadening and zero-frequency signals. The truncation is, however, less efficient if the couplings are of comparable magnitude.

The PDLF spectrum is governed by simple two-spin ^{1}H–^{13}C interactions which lead to a superposition of dipolar doublets. The prerequisite is of course that the ^{13}C spin is rare. Without considering relaxation, the PDLF technique is therefore expected to produce better dipolar resolution for multiple-spin systems than PISEMA. The line broadening due to relaxation is, however, more favorable in PISEMA since the spin-locked magnetization decays with the time constant $T_{1\rho}$. In SLF and PDLF, the magnetization decays are governed by the faster T_2 relaxation. Thus, in systems containing strongly coupled and isolated ^{1}H–^{13}C spin pairs the PISEMA method is expected to provide highest spectral resolution since spin relaxation is the main source of line broadening. For samples rich in protons, the PISEMA spectra will broaden due to multiple dipolar couplings and the resolution may deteriorate below the level achieved by the PDLF experiment. Indeed, the best resolution of the one-bond coupling in chain-deuterated THE5 was observed in the PISEMA spectrum. For fully protonated RufH8O and 5CB, however, the PDLF sequence offers comparable or better dipolar resolution of strong couplings than that provided by PISEMA.

For long-range couplings the PDLF experiment yields superior resolution. Weak dipolar interactions are well resolved in PDLF spectra even in the presence of the much stronger one-bond couplings. In many cases, the long-range dipolar splittings can be determined by direct inspection of the PDLF slices. Another advantage of this experiment is that the CP contact time can be adjusted so that the weakly coupled sites are efficiently polarized. To assign long-range couplings, 3D PDLF-based methods may be employed [5,19].

The dipolar interactions in liquid crystals are partially scaled by the anisotropic molecular motion and, therefore, highly effective and robust long cycle time homonuclear decoupling sequences like BLEW-48 can be incorporated in the PDLF experiment. However, the long cycle of this multiple-pulse sequence could, possibly, limit its application in samples with un-averaged couplings. This is in contrast to the PISEMA experiment where high resolution is achieved with a much shorter pulse train.

4.2. Proton resonance offset effects

Since the PISEMA technique is rather sensitive to the ^{1}H frequency offset [49], it can be difficult to obtain high dipolar resolution in the aromatic and aliphatic regions simultaneously due to differences in the ^{1}H chemical shifts. The scaling factor is also affected by the offset. For this reason, it may be necessary to perform several separate PISEMA experiments with the ^{1}H offset optimized for the best dipolar resolution in different spectral parts. In contrast, the BLEW-48 decoupling sequence used in PDLF is rather tolerant to the ^{1}H resonance offset. This is illustrated in Fig. 7 which shows the experimental splitting for the C_4 carbon in THE5 as a function of the ^{1}H carrier frequency. It is clear that the PDLF method is less sensitive to variations in the ^{1}H frequency as compared to PISEMA. The results of numerical spin dynamics simulations are also included in Fig. 7, and they support the experimental observations. The smallest dipolar linewidths were achieved with offsets corresponding to minimum and maximum scaling factors for PISEMA and PDLF, respectively.

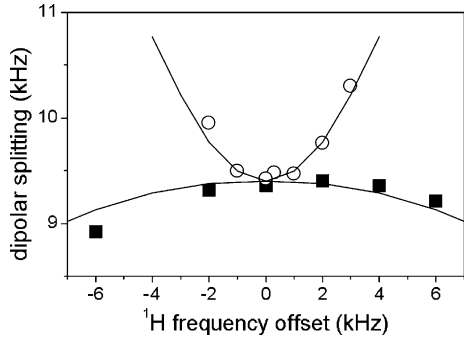

Fig. 7. Splittings for the C_4 carbon in chain-deuterated THE5 obtained at 110 °C versus the ^{1}H carrier frequency. Squares and circles indicate results from PDLF and PISEMA experiments, respectively. The observed dipolar splittings have been divided by the multiple-pulse scaling factors. Results of numerical simulations are also included (solid lines), where a $^1H_4$–$^{13}C_4$ dipolar coupling of 4.70 kHz is used together with the experimental ^{1}H nutation frequencies (see Section 5).

4.3. Radio-frequency heating effects

Limiting the RF heating is important for liquid crystals. Excessive heating can lead to changes of the long-range orientational order, and may even induce phase transitions [50]. The heating effect per unit time is most severe for the PISEMA method where simultaneous high-power irradiation in two RF channels is required during t_1. On the other hand, the high scaling factor in PISEMA results in a relatively short evolution time and therefore in less severe overall sample heating. Moreover, due to the short cycle time of the SEMA sequence, the RF power can be significantly reduced while still maintaining a sufficiently wide spectral width in the dipolar dimension. In practice, we found that the resolution in the aromatic region of 5CB is not affected if the SEMA RF fields are lowered from around 60 to 30 kHz. However, this reduction of field strengths strongly degrades the dipolar resolution for the aliphatic carbons.

All measurements in this work were performed under static (non-spinning) conditions. Previously, local field spectroscopy of liquid crystals has often been combined with off-magic-angle spinning [2,4–6,17–22]. The rapid mechanical sample rotation aligns the director either along or perpendicular to the spinning axis, and leads to scaling of all anisotropic spin interactions [17]. The advantage of OMAS is that lower decoupling fields can be used in order to reduce RF heating. Unfortunately, there are also some inherent drawbacks associated with sample spinning: (i) the dipolar splittings become smaller and this often result in resolution losses and (ii) potential scaling errors are introduced [4,5]. The dipolar resolution is indeed better in the static PDLF spectrum of 5CB shown above as compared to previous results where PDLF experiments were performed under OMAS conditions [6]. Due to the high viscosity, flat temperature dependence of the order parameter and wide temperature range of the mesophase, RF heating causes less problems for columnar phases than for nematic phases. The maximum RF heating observed in this work was in the PISEMA experiment in 5CB, and amounted to approximately 2 °C.

To summarize, we have in this paper studied the performances of the conventional SLF, PDLF and PISEMA methods in various liquid-crystalline systems. It has been shown that the dipolar resolution in the PDLF and PISEMA spectra is up to one order of magnitude better as compared to that observed in conventional SLF experiments. Moreover, the PDLF approach provides in general simpler spectra with higher resolution than those produced by PISEMA. This is particularly clear for weakly coupled spin pairs. The weak sensitivity to ^{1}H resonance offsets also favors the PDLF technique (at least when PDLF is combined with BLEW-48 homonuclear decoupling). The NMR experiments may be performed under stationary conditions with modest sample heating. The advantage of static experiments is that the resolution and accuracy of the measured dipolar couplings is improved as compared to acquiring the local field spectra under OMAS.

5. Experimental

Isotopically labeled THE5 and RufH8O were synthesized according to previously described procedures [51]. The nematic liquid crystal 5CB was obtained from Merck and used without further purification.

All NMR experiments were performed at a magnetic field of 9.4 T on a Chemagnetics Infinity-400 spectrometer equipped with a 6 mm double-resonance MAS probe. Ramped ^{1}H–^{13}C cross-polarization [52] (except for the PDLF sequence where constant-amplitude CP was employed) with nutation frequencies of approximately 50 kHz, and contact times of 1–3 ms was used.

For homonuclear decoupling by BLEW sequences in the SLF and PDLF experiments, the RF field strength was set to $\gamma B_1/2\pi = 75$ and 62 kHz for measurements, respectively, in columnar and nematic phases. In PISEMA during t_1 period, RF field strengths were 50 kHz in the proton and 61 kHz in the carbon channel. Heteronuclear decoupling during the detection period in columnar and nematic phases was achieved by, respectively, 50 and 24 kHz ^{1}H TPPM irradiation [46]. The recycle delays were between 6 and 10 s. Sample heating effects due to RF irradiation was most severe for 5CB. It was calibrated by observing the shift of the nematic-to-isotropic phase transition temperature, and amounted to a maximum of 2 °C.

Numerical simulations were performed using the SIMPSON programming package [53].

Acknowledgments

This work was supported by the Swedish Research Council, the Carl Trygger Foundation, the Magn. Bergvall Foundation, and the Deutscher Akademischer Austauschdienst together with the Swedish Institute under Project No. 313-S-PPP-7/98.

References

[1] R.K. Hester, J.L. Ackerman, B.L. Neff, J.S. Waugh, Separated local field spectra in NMR: determination of structure in solids, Phys. Rev. Lett. 36 (1976) 1081–1083.
[2] K. Schmidt-Rohr, D. Nanz, L. Emsley, A. Pines, NMR measurement of resolved heteronuclear dipole couplings in liquid crystals and lipids, J. Phys. Chem. 98 (1994) 6668–6670.
[3] M. Hong, K. Schmidt-Rohr, A. Pines, NMR measurement of signs and magnitudes of C–H dipolar couplings in lecithin, J. Am. Chem. Soc. 117 (1995) 3310–3311.
[4] S. Caldarelli, M. Hong, L. Emsley, A. Pines, Measurement of carbon–proton dipolar couplings in liquid crystals by local dipolar field NMR spectroscopy, J. Phys. Chem. 100 (1996) 18696–18701.
[5] M. Hong, A. Pines, S. Caldarelli, Measurement and assignment of long-range C–H dipolar couplings in liquid crystals by two-dimensional NMR spectroscopy, J. Phys. Chem. 100 (1996) 14815–14822.
[6] B.M. Fung, K. Ermolaev, Y. Yu, ^{13}C NMR of liquid crystals with different proton homonuclear dipolar decoupling methods, J. Magn. Reson. 138 (1999) 28–35.
[7] P. Palmas, P. Tekely, D. Canet, Local-field measurements on powder samples from polarization inversion of the rare-spin magnetization, J. Magn. Reson. Ser. A 104 (1993) 26–36.
[8] C.H. Wu, A. Ramamoorthy, S.J. Opella, High-resolution heteronuclear dipolar solid-state NMR spectroscopy, J. Magn. Reson. Ser. A 109 (1994) 270–272.
[9] A. Ramamoorthy, C.H. Wu, S.J. Opella, Experimental aspects of multidimensional solid-state NMR correlation spectroscopy, J. Magn. Reson. 140 (1999) 131–140.
[10] R. Fu, C. Tian, T.A. Cross, NMR spin locking of proton magnetization under a frequency-switched Lee–Goldburg pulse sequence, J. Magn. Reson. 154 (2002) 130–135.
[11] P. Caravatti, G. Bodenhausen, R.R. Ernst, Heteronuclear solid-state correlation spectroscopy, Chem. Phys. Lett. 89 (1982) 363–367.
[12] T. Nakai, T. Terao, Measurements of heteronuclear dipolar powder patterns due only to directly bonded couplings, Magn. Reson. Chem. 30 (1992) 42–44.
[13] M. Mehring, J.S. Waugh, Magic-angle NMR experiments in solids, Phys. Rev. B 5 (1972) 3459–3471.
[14] A. Bielecki, A.C. Kolbert, M.H. Levitt, Frequency-switched pulse sequences: homonuclear decoupling and dilute spin NMR in solids, Chem. Phys. Lett. 155 (1989) 341–346.
[15] A. Bielecki, A.C. Kolbert, H.J.M. De Groot, R.G. Griffin, M.H. Levitt, Frequency-switched Lee–Goldburg sequences in solids, Adv. Magn. Reson. 14 (1990) 111–124.
[16] A. Höhener, L. Müller, R.R. Ernst, Dipole-coupled carbon-13 spectra, a source of structural information on liquid crystals, Mol. Phys. 38 (1979) 909–922.
[17] J. Courtieu, J.P. Bayle, B.M. Fung, Variable angle sample spinning NMR in liquid crystals, Prog. Nucl. Magn. Reson. Spectrosc. 26 (1994) 141–169.
[18] B.M. Fung, Liquid crystalline samples: carbon-13 NMR, in: D.M. Grant, R.K. Harris (Eds.), Encyclopedia of Nuclear Magnetic Resonance, Wiley, Chichester, 1996, pp. 2744–2751.
[19] S. Caldarelli, A. Lesage, L. Emsley, Long-range dipolar couplings in liquid crystals measured by three-dimensional NMR spectroscopy, J. Am. Chem. Soc. 118 (1996) 12224–12225.
[20] H. Sun, B.M. Fung, Orientational ordering of a nematic liquid crystal and its mixture with its chain-perfluorinated analogue, Liq. Cryst. 27 (2000) 755–761.
[21] H. Sun, M.D. Roth, B.M. Fung, Orientational ordering in the nematic phase of 4-alkyl-4′-cyanobicyclohexanes, Liq. Cryst. 28 (2001) 1469–1474.
[22] C. Canlet, B.M. Fung, Determination of long-range dipolar couplings using mono-deuterated liquid crystals, J. Phys. Chem. B 104 (2000) 6181–6185.
[23] S.V. Dvinskikh, I. Furó, Order parameter profile of perfluorinated chains in a lamellar phase, Langmuir 16 (2000) 2962–2967.
[24] M. Hong, K. Schmidt-Rohr, DISTINCT NMR for sign determination of C–H dipolar couplings in liquid-crystalline lipids, J. Magn. Reson. Ser. B 109 (1995) 284–290.
[25] M. Hong, K. Schmidt-Rohr, D. Nanz, Study of phospholipid structure by ^{1}H, ^{13}C, and ^{31}P dipolar couplings from two-dimensional NMR, Biophys. J. 69 (1995) 1939–1950.
[26] S. Massou, M. Tropis, A. Milon, Cholesterol in oriented bilayers: determination of the order parameters by proton detected local field NMR spectroscopy, J. Chim. Phys. 96 (1999) 1595–1601.
[27] A. Ramamoorthy, F.M. Marassi, M. Zasloff, S.J. Opella, Three-dimensional solid-state NMR spectroscopy of a peptide oriented in membrane bilayers, J. Biomol. NMR 6 (1995) 329–334.
[28] F.M. Marassi, A. Ramamoorthy, S.J. Opella, Complete resolution of the solid-state NMR spectrum of a uniformly ^{15}N-labeled membrane protein in phospholipid bilayers, Proc. Natl. Acad. Sci. USA 94 (1997) 8551–8556.
[29] F.M. Marassi, S.J. Opella, NMR structural studies of membrane proteins, Curr. Opin. Struct. Biol. 8 (1998) 640–648.
[30] S. Lambotte, P. Jasperse, B. Bechinger, Orientational distribution of α-helixes in the colicin B and E1 channel domains: a one and two dimensional ^{15}N solid-state NMR investigation in uniaxially aligned phospholipid bilayers, Biochemistry 37 (1998) 16–22.
[31] Y. Kim, K. Valentine, S.J. Opella, S.L. Schendel, W.A. Cramer, Solid-state NMR studies of the membrane-bound closed state of the colicin E1 channel domain in lipid bilayers, Protein Sci. 7 (1998) 342–348.
[32] F. Tian, Z. Song, T.A. Cross, Orientational constraints derived from hydrated powder samples by two-dimensional PISEMA, J. Magn. Reson. 135 (1998) 227–231.
[33] F.M. Marassi, J.J. Gesell, A.P. Valente, Y. Kim, M. Oblatt-Montal, M. Montal, S.J. Opella, Dilute spin-exchange assignment of solid-state NMR spectra of oriented proteins: acetylcholine M2 in bilayers, J. Biomol. NMR 14 (1999) 141–148.
[34] S.J. Opella, F.M. Marassi, J.J. Gesell, A.P. Valente, Y. Kim, M. Oblatt-Montal, M. Montal, Structure of the M2 channel-lining segments from nicotinic acetylcholine and NMDA receptors by NMR spectroscopy, Nat. Struct. Biol. 6 (1999) 374–379.
[35] F.M. Marassi, S.J. Opella, A solid-state NMR index of helical membrane protein structure and topology, J. Magn. Reson. 144 (2000) 150–155.
[36] F.M. Marassi, C. Ma, J.J. Gesell, S.J. Opella, Three-dimensional solid-state NMR spectroscopy is essential for resolution of resonances from in-plane residues in uniformly ^{15}N-labeled helical membrane proteins in oriented lipid bilayers, J. Magn. Reson. 144 (2000) 156–161.
[37] Z. Song, F.A. Kovacs, J. Wang, J.K. Denny, S.C. Shekar, J.R. Quine, T.A. Cross, Transmembrane domain of M2 protein from influenza A virus studied by solid-state ^{15}N polarization inversion spin exchange at magic angle NMR, Biophys. J. 79 (2000) 767–775.
[38] J. Wang, J. Denny, C. Tian, S. Kim, Y. Mo, F. Kovacs, Z. Song, K. Nishimura, Z. Gan, R. Fu, J.R. Quine, T.A. Cross, Imaging

membrane protein helical wheels, J. Magn. Reson. 144 (2000) 162–167.
[39] C.S. Nagaraja, K.V. Ramanathan, Determination of order parameters of liquid crystals: use of dipolar oscillations enhanced by Lee–Goldburg decoupling, Liq. Cryst. 26 (1999) 17–21.
[40] N. Sinha, K.V. Ramanathan, Use of polarization inversion for resolution of small dipolar couplings in SLF-2D NMR experiments—an application to liquid crystals, Chem. Phys. Lett. 332 (2000) 125–130.
[41] S.V. Dvinskikh, Z. Luz, H. Zimmermann, A. Maliniak, D. Sandström, Molecular characterization of hexaoctyloxy-rufigallol in the solid and columnar phases: a local field NMR study, J. Phys. Chem. B 107 (2003) 1969–1976.
[42] R.R. Ernst, G. Bodenhausen, A. Wokaun, Principles of Nuclear Magnetic Resonance in One and Two Dimensions, Clarendon Press, Oxford, 1987.
[43] P. Mansfield, Symmetrized pulse sequences in high resolution NMR in solids, J. Phys. C 4 (1971) 1444–1447.
[44] W.-K. Rhim, D.D. Elleman, R.W. Vaughan, Analysis of multiple pulse NMR in solids, J. Chem. Phys. 59 (1973) 3740–3749.
[45] D.P. Burum, M. Linder, R.R. Ernst, Low-power multipulse line narrowing in solid-state NMR, J. Magn. Reson. 44 (1981) 173–188.
[46] A.E. Bennett, C.M. Rienstra, M. Auger, K.V. Lakshmi, R.G. Griffin, Heteronuclear decoupling in rotating solids, J. Chem. Phys. 103 (1995) 6951–6958.
[47] V. Rutar, R. Blinc, M. Vilfan, A. Zann, J.C. Dubois, ^{13}C NMR study of molecular ordering in a discotic columnar mesophase, J. Phys. (Paris) 43 (1982) 761–765.
[48] M. Werth, J. Leisen, C. Boeffel, R.Y. Dong, H.W. Spiess, Mobility changes of side chains ascribed to density modulations along columnar structures detected by 2D NMR, J. Phys. II France 3 (1993) 53–67.
[49] Z. Gan, Spin dynamics of polarization inversion spin exchange at the magic angle in multiple spin systems, J. Magn. Reson. 143 (2000) 136–143.
[50] B.M. Fung, ^{13}C NMR studies of liquid crystals, Prog. Nucl. Magn. Reson. Spectrosc. 41 (2002) 171–186.
[51] H. Zimmermann, Specifically deuterated intermediates for the synthesis of liquid crystals and liquid-crystalline polymers, Liq. Cryst. 4 (1989) 591–618.
[52] G. Metz, X. Wu, S.O. Smith, Ramped-amplitude cross polarization in magic-angle-spinning NMR, J. Magn. Reson. Ser. A 110 (1994) 219–227.
[53] M. Bak, J.T. Rasmussen, N.C. Nielsen, SIMPSON: a general simulation program for solid-state NMR spectroscopy, J. Magn. Reson. 147 (2000) 296–330.